# A Controlled Evaluation of Tuned-Aperture Computed Tomography Applied to Digital Spot Mammography

Richard L. Webber, Hunter R. Underhill, and Rita I. Freimanis

**The purpose of this work was to compare the detection accuracy of 3-dimensional (3D) modalities of tuned-aperture computed tomography (TACT) with that of conventional 2-dimensional (2D) digital spot mammograms. A standardized mammographic phantom was placed beneath cadaveric breast tissues of varying densities. Five radiologists were asked to detect as many objects (specks, fibers, and low-contrast masses) as possible from 90 displays in a controlled and factorially balanced multivariate experiment. Radiographic exposure was varied systematically, and projections were averaged to ensure stochastic comparability. Scores were weighted to eliminate task-specific bias and were analyzed by multivariate analyses of variance. All display modalities based on the linear application of the 3D TACT reconstruction method yielded significantly higher detection scores for all tasks than did conventional 2D digital spot mammography, which served as the scientific control modality. This effect was found to be statistically significant ($P < .001$) in spite of significant variations between tissues ($P < .001$), observers ($P < .001$), and exposures ($P < .01$). TACT may be a promising alternative or enhancement to conventional 2D digital mammography for tasks well simulated by this experimental design.**



**KEY WORDS: computed tomography, three-dimensional, observer performance, digital radiography, breast radiography, tomosynthesis.**

AS PRACTICED CURRENTLY, mammography is a 2-dimensional (2D) imaging process limited by overlap of normal tissue that obscures diagnostic information, as illustrated by the fact that abnormalities are easier to detect in fatty breasts than in dense ones.[1,2] The addition of depth information via conventional stereometry has been shown to improve diagnostic performance.[3] However, this approach does not allow for suppression of 3-dimensional (3D) details known to be irrelevant (structured noise).[4] Conventional computed tomography (CT) lacks the high resolution needed for mammographic tasks.[5] Recent findings by Niklason et al[6] suggest that digital tomosynthesis offers many potential benefits for breast cancer screening. These benefits include improved specificity and sensitivity through reduction of structured noise and accommodation to realistic design constraints.

This investigation explores the potential benefits of tuned-aperture computed tomography (TACT), a new digital 3D imaging technique.[7] Although similar to tomosynthesis in that it creates tomographic slices from a series of 2D projections, TACT is much more forgiving and flexible. Its reconstruction method is derived from *a posteriori* analysis of projected data rather than from algorithms requiring *a priori* restriction of projection geometry.[8,9]

## TACT, TOMOSYNTHESIS, AND APERTURE THEORY

In many ways, the locus of x-ray source positions associated with circular tomosynthesis can be considered an analogue of the numerical aperture associated with conventional lens systems. For example, when the locus of source positions approaches a single point (as is the case in transmission radiography), the optical behavior of the associated "aperture" is well described by images produced from a pinhole camera. This is to say that both transmission radiographs and images projected through a pinhole have infinite depth of field. Conversely, a relatively narrow depth of field characterizes tomographic slices, which are produced from multiple source points distributed over a large region in close proximity to the irradiated object. In this respect, they simulate the optical characteristics of an image produced by a camera having a relatively large numerical aperture. Just as the maximum angle subtended at a point in space by a camera lens determines the resulting depth of field, the maximum angle subtended at a fixed position in a radiographed object by an extended

*From the Wake Forest University School of Medicine, Winston-Salem, NC.*

*This research was supported in part by a technology development grant from North Carolina Baptist Hospital (No. NCBH A0195) and two grants from the National Institutes of Health (NIH 5 RO1 CA 7416-02 and NIH Training Grant 5 T35 DK-07400-19).*

*TACT is a registered trademark for Tuned-Aperture Computed Tomography.*

*Address reprint requests to Richard L. Webber, DDS, PhD, Department of Dentistry, Wake Forest University School of Medicine, Medical Center Blvd, Winston-Salem, NC 27157-1093.*



*0897-1889/00/1302-0005$10.00/0*
*doi:10.1053/di.2000.5423*

locus of point-source positions determines the so-called tomosynthetic slice thickness. In both examples, the size of the effective "aperture" determines the depth of field such that the greater the subtended angle, the narrower the region of relative focus measured in the third dimension.

Taking the analogy a bit further, consider the photographic advantages made possible by attaching an iris diaphragm to a camera lens. A photographer is now free to adjust the f-stop of a camera and thereby control the resulting depth of focus in ways that optimize a particular photographic objective. In effect, TACT provides the same flexibility in tomosynthetic applications. By accommodating arbitrary projections from any angle, TACT allows an x-ray technician to adjust individual radiation trajectories in task-specific ways. This purposeful adjustment of the aperture of an equivalent "x-ray camera" led to the name "tuned-aperture computed tomography."

This intrinsic tomosynthetic flexibility also extends beyond the photographic limitations imposed by an optical system. Unlike a camera lens, the virtual aperture of a TACT system is not open all at the same time during an exposure. Rather, it is synthesized one point at a time from individual projections exposed separately from different angles. Under these conditions, patient movement during sufficiently short exposure times is equivalent only to a slight variation in projection geometry. Therefore, the effects are no more significant than a modest change in the size of the aperture of an analogously shaped camera lens. In other words, with TACT, rigid structures of diagnostic interest can be moved freely between exposures with impunity, unlike the situation with conventional tomosynthesis and CT.

Like tomosynthesis, TACT suppresses diagnostically irrelevant 3D tissue details, and it can be realized by using mammographic digital-imaging hardware currently available for spot mammograms. The approach is similar to that used for stereomammography[10] and can be accommodated with existing technical resources and related clinical expertise. The result is a tomographic display that can be manipulated interactively after acquisition of an arbitrary series of discrete exposures from multiple angles. The projection geometry may be confined to a single sweep spanning a limited angle oriented in a plane parallel to the chest wall of the patient. An associated potential advantage is slice selection that facilitates visualization of details buried in overlying tissues without the need for extreme compression, which otherwise is required to disperse the tissues for optimal 2D display and is sometimes painful.

The intent of this study was to test this imaging method on a variety of simulated diagnostic tasks using a standardized digital calibration phantom as the "gold standard." Specifically, the following multivariate null hypothesis was tested:

When comparing TACT and conventional digital spot mammograms, differences in radiographic detectability of various standardized structural details obscured by natural breast tissues are independent of (1) modalities of display (both 2D and 3D, linear, and nonlinear), (2) breast density, (3) type of detail, (4) radiographic exposure, and (5) observer.

## MATERIALS AND METHODS

Fresh, normal-appearing breasts were amputated from 6 cadavers. These unembalmed specimens were positioned between 2 parallel plates, as with modest amounts of clinical mammographic compression. The specimens then were fast frozen in their compressed shapes, and the plates removed for radiography. Conventional film-screen mammograms were taken of each frozen specimen. Portions of these breasts were chosen so as to yield 3 fatty areas and 3 dense areas, with varying degrees of fibroglandular density.

The frozen breasts were hemisectioned axially to render a thinner specimen having an unbiased distribution of tissue patterns. The total attenuation contributed by breast tissues was thereby reduced to that which permitted detection of the least challenging test objects simulated in this study. The test objects were those contained in the wax insert of a digital mammography evaluation phantom (Model 18-250; Nuclear Associates Division, Victoreen, Inc, Carle Place, NY): specks, fibers, and masses organized in a standardized pattern of decreasing size within each group. This insert was placed in turn under the chosen portions of the hemisectioned frozen breasts to yield a series of 6 phantom/breast combinations. When radiographed with conventional digital spot technique and viewed on a monitor, the resulting images from these hybrid phantoms resembled clinical mammographic spot films characterized by various tissue densities containing known "lesions" (Fig 1).

Appropriate beam qualities were selected for each phantom/breast combination through visual inspection of computer displays after assessment of the effects of changes in window and level settings. A comprehensive series of displays was produced by systematic variation of kVp throughout the interpretable range. The kVp values associated with the single best image in each series were chosen, maximizing contrast without brightness clipping of details. The resulting images were confirmed as being appropriate by an FDA-certified radiologist who specializes in mammography. Exposure was fixed at a reasonably high value (63 mAs) across all specimens to provide a uniform baseline for subsequent systematic changes in exposure. This constraint had no significant biasing effect on image

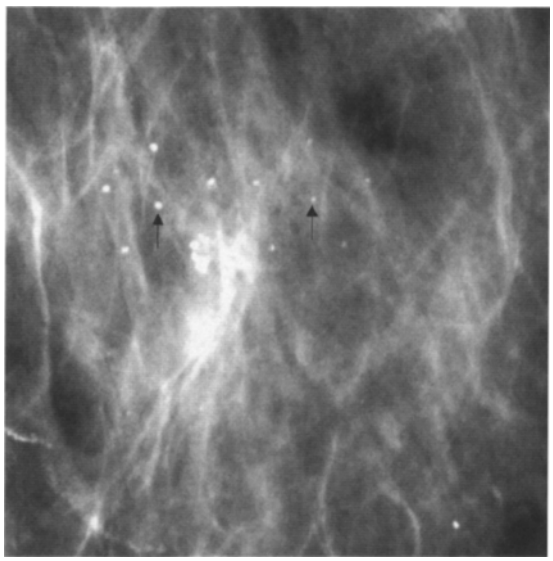

**Fig 1. Conventional digital spot mammographic image of hybrid phantom (frozen breast tissue and evaluation phantom insert) shows speck clusters ("lesions") of phantom insert (arrows).**

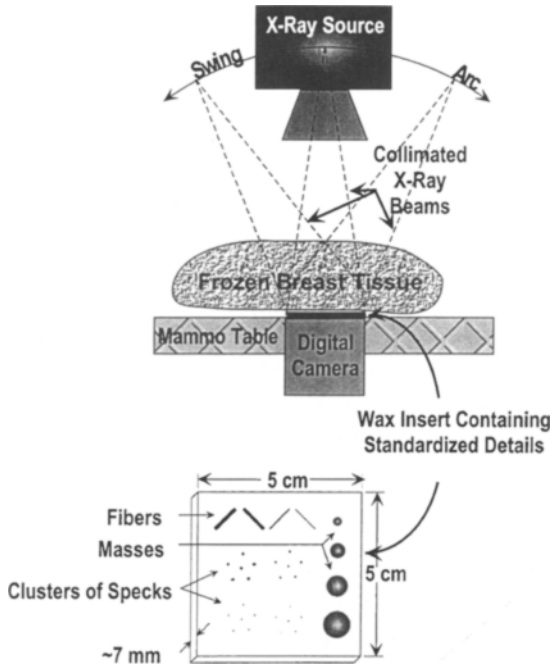


**Fig 2. Projection geometry and phantom details.**

quality because the solid-state imager is relatively linear (unlike mammographic film). All images were produced with a commercial mammographic x-ray machine configured for digital biopsy applications (Delta 16; Instrumentarium Imaging, Tuusula, Finland). The settings are shown in Table 1. The wax insert of the phantom is the same size and shape (5 cm × 5 cm) as the detector in the digital x-ray machine, and therefore was displayed at its full resolution.

To generate the experimental sets of TACT images, we obtained 7 exposures of each specimen by moving the swing arm containing the tube head in an arc (Fig 2). The resulting mammographic projections had angular disparities of −15°, −10°, −5°, 0°, 5°, 10°, and 15° from vertical. For each specimen's control image, we acquired another series of 7 exposures at identical settings, this time at 0° with respect to the vertical, and averaged them to assure a comparable signal-to-noise ratio (SNR) between tomosynthetic test and conventional control modalities.

A second set of test and control images was obtained with the mAs reduced by nearly one half (32 mAs). Finally, the mAs was again reduced by one half (16 mAs), and a third set of images was generated. The purpose of these systematic exposure reductions was to evaluate detection performance under conditions approaching the quantum limit for each task.

**Table 1. Optimized kVp and Fixed mAs for Each Specimen**

| Specimen | Thickness (cm) | Density | kVp | mAs | | |
|---|---|---|---|---|---|---|
| | | | | High | Medium | Low |
| 1 | 1.8 | Fatty | 24 | 63 | 32 | 16 |
| 2 | 1.7 | Fatty | 23 | 63 | 32 | 16 |
| 3 | 1.9 | Fatty | 24 | 63 | 32 | 16 |
| 4 | 1.3 | Dense | 22 | 63 | 32 | 16 |
| 5 | 1.4 | Dense | 24 | 63 | 32 | 16 |
| 6 | 1.2 | Dense | 21 | 63 | 32 | 16 |

The various multiangle test groups were converted to a series of tomosynthetic slices distributed throughout the specimens using 3 different modalities (algorithms). The first modality was a linear method called back projection, which shifts and averages the individual 2D projections. The end product is a series of focal planes (slices) that pass through the specimen at different depths. Objects that lie in a given focal plane are seen clearly; objects above or below this plane are blurred. To reduce the amount of artifactual blurring, these data were processed further using a second linear modality, which involves the application of an iterative deconvolution process known to eliminate tomosynthetic artifacts produced by structures lying outside the focal plane.[11] A 3D deconvolution based on the known point-spread function produced by the individual projections was performed once and then 2 more times. This provides balanced data with the potential to demonstrate performance differences based on the inevitable build-up of uncorrelated noise associated with iterative processes. The third and final tomosynthetic modality was a new and highly nonlinear slice synthesis method (minimization) designed to maximize task specificity, albeit at the expense of detection sensitivity.[12]

The test modalities resulted in a control image, an average-value slice produced by simple back projection, a back-projected slice deblurred by a single restorative iteration (1×), a back-projected slice comparably deblurred by 3 iterations (3×), and a nonlinearly computed slice (Fig 3). From each of the tomosynthetic series, computer displays were produced at 3 different exposure levels (mAs). This process yielded a total of 90 images (72 test, 18 control) uniformly distributed among all the independent variables in a balanced factorial design. All displays were scaled identically and reflect the intrinsic resolu-

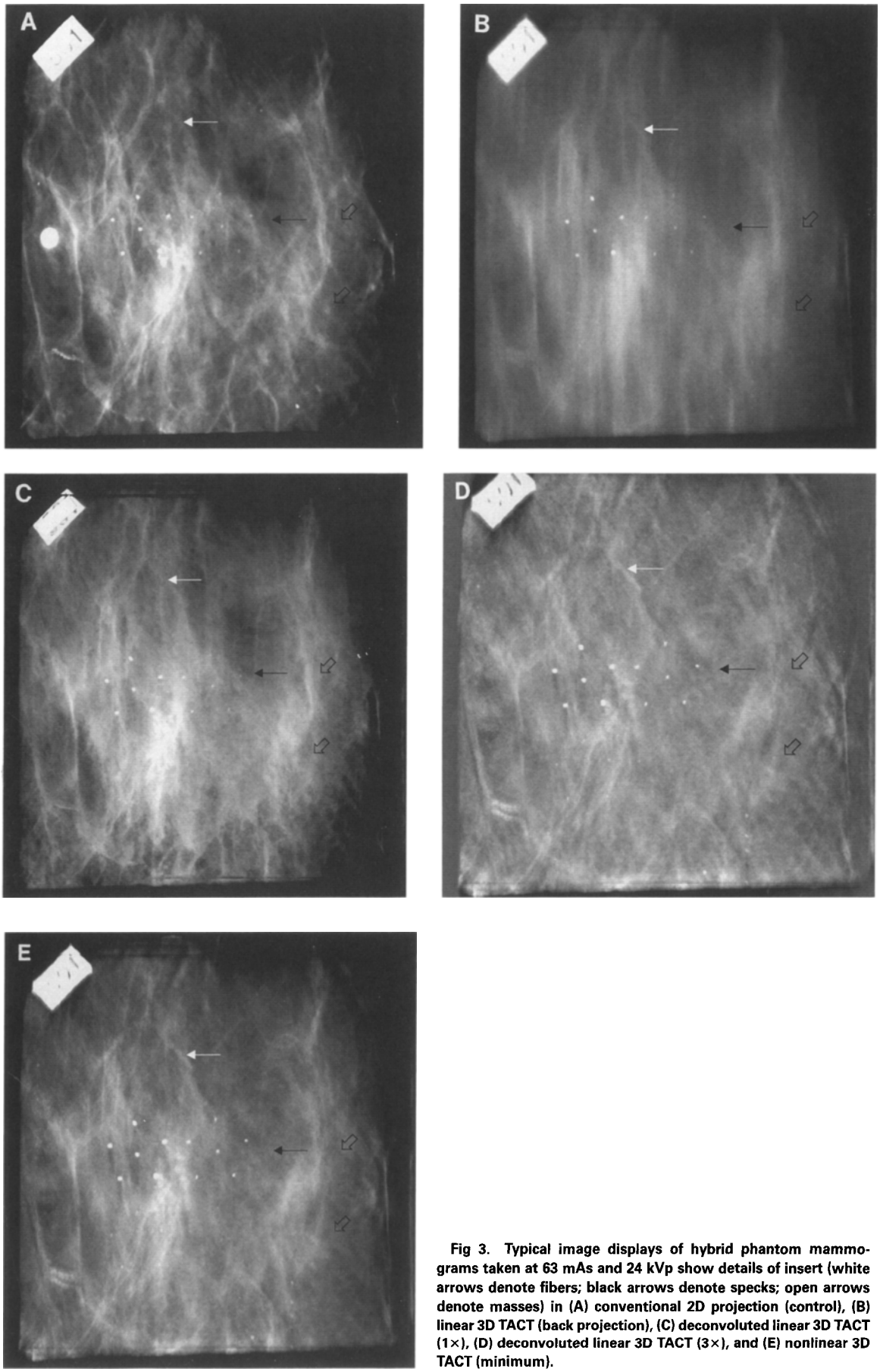


**Fig 3. Typical image displays of hybrid phantom mammograms taken at 63 mAs and 24 kVp show details of insert (white arrows denote fibers; black arrows denote specks; open arrows denote masses) in (A) conventional 2D projection (control), (B) linear 3D TACT (back projection), (C) deconvoluted linear 3D TACT (1×), (D) deconvoluted linear 3D TACT (3×), and (E) nonlinear 3D TACT (minimum).**

tion of the digital sensor (1,024 pixels × 1,024 pixels) distributed uniformly across a square region measuring 5 cm on each side, yielding a pixel length of 48.8 μm.

The viewing sequence of these 90 images was randomized and the images flipped between observers to prevent possible learning effects or other sequence-specific sources of potential bias. Four FDA-certified mammography-interpreting physicians and one mammography fellow viewed all images in a darkened room. Displays were shown at full resolution on a computer monitor (P1100 series; Hewlett-Packard, Boise, Idaho) as monochromatic images with a dynamic range of 8 bits (256 gray levels). The monitor itself was oversized (1,600 × 1,200 pixels), and its 75-Hz refresh rate was well above the observer's flicker fusion frequency at the brightness settings selected for data display. The window and level settings of these electronic images were determined at the time of exposure using the explicit selection criteria described earlier. The monitor's display was degaussed, and adjusted for geometric linearity and for proper convergence before observer participation. Although somewhat restrictive, this fixed experimental design eliminated any possibility of observer bias affecting the way information was presented. It also introduced no significant conceptual problems because all performances were evaluated relative to control projections that were displayed under comparable conditions.

All observers were trained before testing by means of a tutorial with verbal feedback based on a set of 10 representative images. Both a radiograph of the wax phantom insert and a schematic diagram illustrating all possible spatial arrangements of the wax insert were available to aid in visualizing the configuration of the details in each individual computer image. This precaution assured that the configuration of details on the ACR phantom was well known to all the observers, effectively precluding opportunities for false-positive findings. The observers were asked to identify, respectively, the number of specks, fibers, and masses in each display that, in their judgments, were considered radiographically detectable. Hence, this experimental design assured specificities approaching 100% and discriminated among the variables solely on the basis of measured differences in sensitivity scores. The number of test objects of each type detected by the radiologists was recorded for each image. If any part of the detail could be recognized, then the entire object was considered detected. To compensate for the 6 specks of equal size in each group, the reported scores for fibers and masses were weighted by a factor of 6.

## RESULTS

A multivariate analysis of variance was used to test the null hypothesis. This hypothesis was rejected for every independent variable covered in the underlying balanced factorial design. These results, including all significant interactions, are detailed in Table 2.

The significant modality effects may be the most clinically interesting because of their potential for improving diagnostic performance. Subsequent statistical comparison of detection using various modalities indicated that significant results were derived from all three linear TACT-based tomosynthetic reconstruction schemes. *These modalities were superior to those produced by the conventional control for all three tasks at all exposures for all tissue densities and for all observers.* Moreover, this relationship was preserved even when the effects of exposure only were optimized for the control as seen by the mean scores (Fig 4). When we applied Scheffé's post hoc multiple comparisons test, we found that even under these extreme conditions, all three linear TACT-based tomosynthetic reconstruction schemes were significantly different from the control ($P < .05$). However, the same test indicated that performance differences between the 3 linear TACT-based reconstructions were not significantly different from each other.

**Table 2. Statistical Significance From Factorial ANOVA by Independent Variable**

| Source of Variation | DF | F Ratio | *P* Value |
|---|---|---|---|
| Main effects | 13 | 320.31 | <.001 |
| Modality | 4 | 365.48 | <.001 |
| Density | 1 | 353.08 | <.001 |
| Exposure | 2 | 39.53 | <.010 |
| Observer | 4 | 20.36 | <.010 |
| Task | 2 | 1094.26 | <.001 |
| Significant 2-way interactions | 64 | 7.64 | <.001 |
| Density and mode | 4 | 2.41 | <.050 |
| Density and task | 2 | 28.91 | <.010 |
| Exposure and task | 4 | 10.73 | <.001 |
| Modality and task | 8 | 40.51 | <.010 |
| Observer and task | 8 | 3.84 | <.001 |
| Significant 3-way interaction | 148 | 1.35 | <.010 |
| Density, modality, and task | 8 | 13.60 | <.005 |

We also explored the effect of breast density to confirm that it is consistent with the clinical perception that fatty breasts are less likely to obscure diagnostic details than are more dense tissues. The associated difference in mean scores shown in Table 3 confirms this prediction. Variations in x-ray exposure produced another effect of statistical significance. Scores shown suggest that performance was influenced by stochastic noise associated with quantum-limited (low) exposures.

The observed interaction in Table 2 between modality and task was explored to determine whether it might be influenced by the task-specific nature of the nonlinear method. Results tallied in Table 3 present statistically significant differences produced using the nonlinear method and the control at all exposure levels. When respective performance levels were compared by object class, the control was significantly better for speck detec-

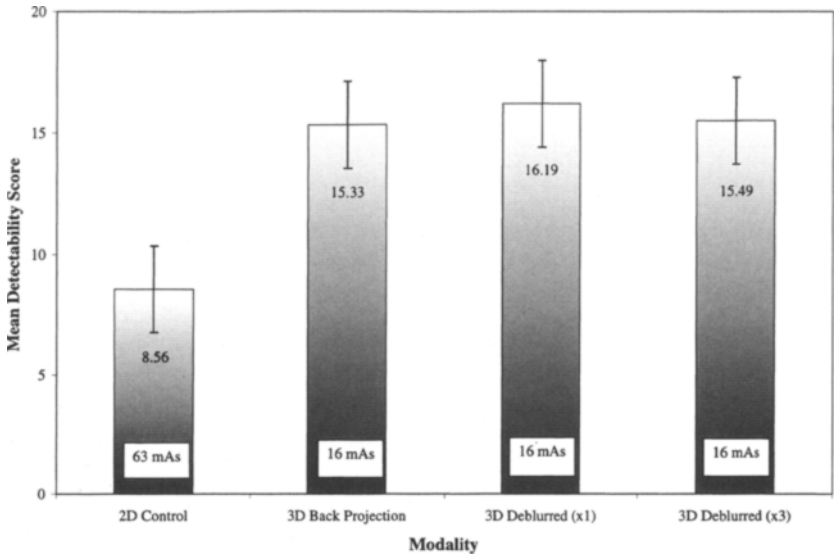


**Fig 4. Performance scores at selected exposures by reconstruction modality. The difference between 2D and 3D modalities is statistically significant ($P < .0001$). Bars indicate ± standard errors.**

tion, but the nonlinear scheme yielded better scores when fibers and masses were the objects of interest.

A possible interaction between exposure and modality was examined statistically from the data shown in Fig 5. The observed trend conforms to the theoretical prediction that the accumulation of uncorrelated noise with increasing numbers of iterations may influence detection adversely, especially at relatively low exposures, at which quantum mottle may be limiting task performance. However, performance differences observed under these conditions were not large enough to yield statistical significance.

The final interaction explored was the one observed between exposure and task (Table 2). Here we predicted that quantum-limited displays (low exposure) would more likely influence the detection of specks and fibers than of masses because masses are large enough to minimize the effects of obscuration by quantum mottle. This hypothesis was found to be consistent with the associated mean scores, as shown in Fig 6.

**Table 3. Selected Performance by Variable**

| Variable | Task(s) | Mean Score |
|---|---|---|
| Tissue type | All | |
| Fatty | | 16.0 |
| Dense | | 11.4* |
| Exposure | All | |
| High (63 mAs) | | 14.9 |
| Medium (32 mAs) | | 14.0 |
| Low (16 mAs) | | 12.2* |
| Modality | | |
| 2D control | Specks | 16.9 |
| 3D nonlinear method | Specks | 15.6* |
| 2D control | Fibers, masses | 2.9* |
| 3D nonlinear method | Fibers, masses | 5.1 |

*Scores are significantly different at $P < .05$.

## DISCUSSION

All linearly derived tomographic TACT image displays significantly increased the detectability of simulated mammographic details relative to conventional transmission-based mammography. This observation is remarkable because of TACT's relative independence from all the other significant interactive effects listed in Table 2. This is to say that its demonstrated superiority was not obviated by the

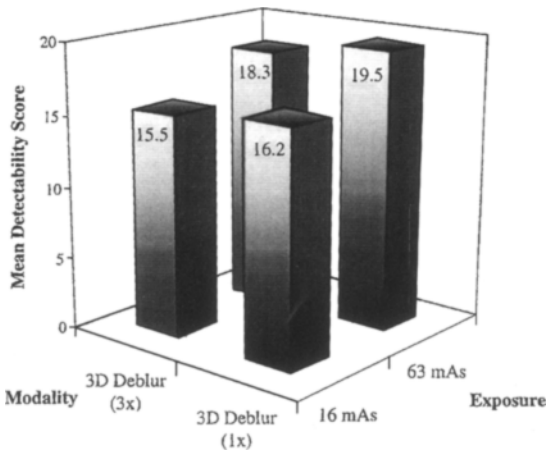


**Fig 5. Performance matrix by amount of iterative deblurring and exposure. The differences between deblurring modalities are not statistically significant.**

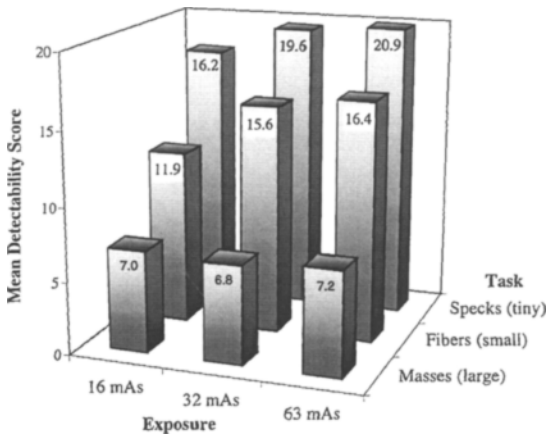


**Fig 6. Performance matrix by task and exposure. Extreme differences in both directions are statistically significant.**

particular detection task performed, by which observer made the assessment, by variations in breast density, or by the x-ray exposure level. Exposure was prorated across all 7 TACT projections, so that it was no greater than that used to produce the control mammogram. Thus, the significantly improved performance observed for the linear TACT modalities relative to the conventional digital control (Fig 4) was achieved with a nearly fourfold reduction in exposure.

Use of the well-known ACR standard phantom in this study precludes objective determination of false-positive findings. However, there is no 3D mammography phantom with the professional acceptance of the ACR standard, which is suitable for this project and would allow determination of specificity. Clearly, science would benefit from the development of a more appropriate and sophisticated 3D mammographic phantom for investigations of this sort.

The significant effect of tissue density (Table 3) confirms the clinical observation that dense breasts can hide important diagnostic details. Because this effect was found to influence detection differently, depending on task, modality, and exposure, it is important to consider all these interactive factors in any practical mammographic system based on related technology.

The negative effect of reduced exposure was not unexpected, considering the relatively low photon fluences involved and the fact that certain test objects (specks) had the same relative size as the signals created by individual quantum events. Performance falls off uniformly with decreasing exposure for the speck- and fiber-detection tasks but is relatively uninfluenced by comparable conditions during the mass-detection task.

Related reasoning can be applied to account for the performance disparity observed between the nonlinear modality and the conventional mammographic 2D control for various tasks (Table 3). Here the explanation derives from the fact that the nonlinear method selectively excludes blurring artifacts caused by radiopaque structures at the expense of some loss in SNR. As discussed above, SNR is likely to be most limiting in displays of specks obscured by quantum mottle. These are precisely the displays that were not associated with performance superior to that of the control for nonlinearly processed images. Conversely, for tasks characterized by larger regions of interest (such as the larger fibers and masses), we see benefit from use of the nonlinear method, which eliminates many of the more massive fixed-pattern artifacts produced by linear back-projection algorithms.

Performance among observers differed significantly. Such differences are neither surprising nor of interest here because in most clinical applications the observers are likely to differ in training, experience, and other important but uncontrollable ways. We included this in our analysis only to demonstrate that improvements having significant potential for application must be robust enough to eclipse largely unavoidable variance sources of this sort.

In preparing the test images, we selected only the focal plane centered in the region containing the details in the wax insert. The depth of one region of interest relative to that of another can be measured by simply counting the number of slices of known thickness between the respective regions in best focus. Hence, the 3D methods examined in this study not only provide substantially more information about what is present in each focal plane but also can be used to locate regions of interest volumetrically with no increase in production time, expense, or exposure. This is an added bonus that clearly is unobtainable from the 2D (control) method and has potential for precise localization of lesions within the breast parenchyma or skin for purposes of biopsy or analysis.

We were unable to demonstrate significant differences in performance derived from all linear TACT imaging modalities. This suggests that accumulations of uncorrelated noise associated with multiple

iterations of deblurring may offset the theoretical improvements in image quality made possible by appropriate deconvolution.

To the extent that this approach clarifies visual details known to be representative of those associated with cancerous lesions, this technology could facilitate earlier diagnosis with improved prognosis and reduced mortality. By identifying multiple lesions, it may make possible more accurate assessment of the extent of the disease. Thus, the scope of therapeutic options available may be clarified, and the need for mutilating surgery may be reduced as well.[13]

The superiority of TACT over conventional mammography for detection tasks as simulated in this experiment appears unequivocal from the results of this investigation. However, it is important to recognize that the diagnostic tasks explored were derived from a series of hybrid in vitro mammography specimens and were observed under conditions that may not represent an actual clinical situation. Ideally, a model that more closely simulates breast tissue containing realistic lesions located at different positions and depths, and one that can be altered selectively to facilitate a more balanced experimental design, should be created and tested. It also follows that if this technology were to find significant use as a screening tool in anticipated full-field digital mammography applications, it would be important for it to be evaluated further under conditions designed explicitly to measure specificity as well as sensitivity.

In the meantime, the positive results of this study suggest that TACT imaging may prove a practical alternative to conventional spot mammography (where sensitivity is of primary importance) in applications well simulated by the model investigated here.

## ACKNOWLEDGMENTS

The authors thank Johanna R. Jorizzo, MD, Sherry L. Pulaski, MD, E. Thomas Pulaski, MD, and Gioia J. Riccio, MD, for their contributions as observers. The authors are also grateful to Instrumentarium Imaging for the loan and special modification of the digital stereotactic mammography machine used in this investigation.

## REFERENCES

1. Tabár L, Dean PB: Basic principles of mammographic diagnosis. Diagnostic Imaging Clin Med 54:146-157, 1985

2. Sickles EA: Findings at mammographic screening on only one standard projection: Outcomes analysis. Radiology 208:471-475, 1998

3. May M: Three-dimensional mammography. Am Scientist 82:421-422, 1994

4. Kundel HL, Revesz G: Lesion conspicuity, structured noise, and film reader error. AJR 126:1233-1238, 1976

5. Karssemeijer N, Frieling JTM, Hendriks JHCL: Spatial resolution in digital mammography. Invest Radiol 28:413-419, 1993

6. Niklason LT, Christian BT, Niklason LE, et al: Digital tomosynthesis in breast imaging. Radiology 205:399-406, 1997

7. Webber RL, Horton RA, Tyndall DA, et al: Tuned-aperture computed tomography (TACT). Theory and application for three-dimensional dento-alveolar imaging. Dentomaxillofac Radiol 26:53-62, 1997

8. Webber RL, inventor; Wake Forest University, assignee: Self-calibrated tomosynthetic, radiographic-imaging system, method and device. US patent 5,359,637, October 25, 1994

9. Webber RL, inventor; Wake Forest University, assignee: Self-calibrated tomosynthetic, radiographic-imaging system, method and device. US patent 5,668,844, September 16, 1997

10. Bolmgren J, Jacobson B, Nordenstrom B: Stereotaxic instrument for needle biopsy of the mamma. AJR 129:121-125, 1977

11. Ruttimann UE, Gröenhuis RAJ, Webber RL: Restoration of digital multiplane tomosynthesis by a constrained iteration method. IEEE Trans Med Imaging MI-3:141-148, 1984

12. Webber RL, Underhill HR, Hemler PF, et al: A nonlinear algorithm for task-specific tomosynthetic image reconstruction, in Dobbins JT, Boone JM (eds): SPIE Medical Imaging 1999: Physics of Medical Imaging. San Diego, CA, SPIE, February 1999, pp 258-265

13. Sadowsky NL, Semine A, Harris J: Breast imaging. A critical aspect of breast conserving treatment. Cancer 65:2113-2118, 1990